CRITICAL SPEEDS OF ROTORS BY TRANSFER FINITE ELEMENT METHOD

by

SUDHANSHU GOEL

DEPARTMENT OF MECHANICAL ENGINEERING
INDIAN INSTITUTE OF TECHNOLOGY KANPUR

AUGUST 1986

CRITICAL SPEEDS OF ROTORS BY TRANSFER FINITE ELEMENT METHOD

A Thesis Submitted

In Partial Fulfilment of the Requirements

for the Degree of

MASTER OF TECHNOLOGY

by

SUDHANSHU GOEL

to the

DEPARTMENT OF MECHANICAL ENGINEERING

INDIAN INSTITUTE OF TECHNOLOGY KANPUR

AUGUST, 1986

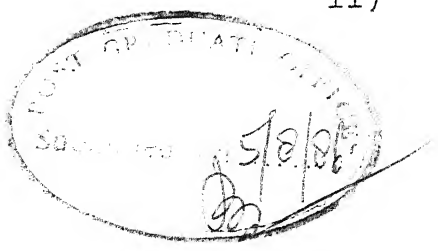

CERTIFICATE

This is to certify that the work entitled, "CRITICAL SPEEDS OF ROTORS BY TRANSFER FINITE ELEMENT METHOD" done by Mr. Sudhanshu Goel has been carried out under my supervision and has not been submitted elsewhere for a degree.

Bhupinder Pal Singh

IIT Kanpur

July, 1986

Bhupinder Pal Singh
Assistant Professor
Department of Mechanical Engineering
Indian Institute of Technology, Kanpur

CONTENTS

LIST OF TABLES

LIST OF FIGURES

NOMENCLATURE

d	:	Diameter
k	:	Radius of gyration
k'	:	Shear averaging coefficient
m	:	Mass per unit length
z	:	Complex Displacement ($= x + iy$)
A	:	Area of cross-section
E	:	Young's modulus
G	:	Shear Modulus
H	:	Non-dimensional length of finite element
I	:	Moment of inertia about diameter of disc
L	:	Rotor length
M_c	:	Material constant
M_x, M_y	:	Moments in different planes
Re	:	Rotary inertia effect factor
S	:	Non-dimensional axial coordinate
S_x, S_y	:	Shear forces in different planes
T_*	:	Characteristic time
Z	:	Non-dimensional complex displacement
ρ	:	Density
η	:	Non-dimensional coordinate along finite element lengt
ω	:	Rotor speed (dimensional)
Ω	:	Rotor speed (Non-dimensional)
Ψ_x, Ψ_y	:	Slopes due to bending moments
$\{\ \}$	:	Column matrix
$[\ ]$	:	Row matrix
$[\ ]$	:	Square matrix

ABSTRACT

Evaluating natural frequencies and critical speeds of rotors is an important problem since these are integral components of many machines.

Transfer Finite Element Method has been used in the present work for determining natural frequencies and critical speeds of rotors taking into account shear deformation, rotary inertia, and gyroscopic action effects. This method offers the advantage of reduced computer memory requirements vis-a-vis standard Finite Element Method. A variety of situations are considered and results are found to be satisfactory.

CHAPTER 1

INTRODUCTION

Dynamics of rotating shafts, rotor dynamics for short, is an important area in the field of mechanical engineering by virtue of the fact that rotors are an integral part of all a turbo-machines and also find use in many other machines.

Modern machines frequently use 'high-speed', also called 'flexible', rotors. These are rotors running at speeds above critical which marks the phenomenon of unacceptably large transverse vibrations and whirling. A complete understanding of the dynamics of such a rotor would involve an understanding of the shaft behaviour in terms of critical speeds, behaviour i post-critical speed regions, the stresses developed, interactio between supports and the shaft, the effects of material damping and resistance between shaft and bearings, etc. A complete analysis of these phenomena is obviously beyond the scope of a work such as the present one.

Since the 1870's when flexible shaft theory first made its appearance in connection with the then novel turbine techniques [1] much work has been done on various aspects of rotor dynamics. Research on the phenomenon of shaft vibrations was initiated by Rankine and Laval in the last quarter of the nineteenth century [1] . A.Stodola, an eminent turbine expert, carried out investigations on many fundamental phenomena in the

early part of this century. More recently, Dimentberg [1] and Tondl [2] have published excellent works on rotor dynamics. Rao [3] has discussed, amongst other things, shaft and fluid-film bearing interaction at length.

The present work focusses attention on a specific area - viz. finding the natural frequencies and critical speeds of rotors under various conditions. The specific problems address are:

i) uniform rotors with different boundary conditions
ii) non-uniform rotors
iii) rotors with in-span supports

Problems of this nature have, ofcourse, been solved earlier using different methods. (Section 1.1 outlines some of the more important ones). The present work applies the Transfer Finite Element technique [4] for solving the problems mentioned above. Some notes on the Transfer Finite Element Method are given in Section 1.2. Different FORTRAN programs have been developed to obtain values of critical speeds for different rotor systems.

It is highly advantageous to work with nondimensionalised variables of space and time for it makes the results very general. The results become applicable to shafts which are different physically but have the same nondimensional parameters. The governing differential equations have therefor

nondimensional quantities.

1.1 Methods of Analysis

The methods generally used for finding natural frequencies of transverse vibrations can be grouped broadly under the following heads:

i) Exact (closed-form) solutions

ii) Approximate methods.

Some of the popular methods in these categories are mentioned here.

i) Exact Solutions: The earliest efforts at determini natural frequencies of rotors treated the shaft as an Euler beam [5]. Indeed, if the effects of rotary inertia, shear deformation, and gyroscopic action of discs and rotor elements are neglected, the problem does reduce to one of an Euler beam. Making these assumptions, then, it is possible to obtai an exact expression for natural frequencies from the governing differential equations of the system.

Dimentberg [1] has obtained closed form solution for a simple-simple rotor considering all the effects mentioned above. There are, however, two major limitations: (i) result can be obtained only for simple rotor configurational geometri and (ii) determining of the frequency equation is a very tedious job specially if the end conditions are not simple.

Gyroscopic action of a disc mounted on a shaft is considered in many texts [1,3,6,7] . In all these cases, however, the rotor itself is considered massless and effects of rotor elements are ignored.

Patnaik and Mallik [8] have investigated the natural frequencies of a rotor with lumped inertias considering the mass of the rotor also. They consider a rotor on multiple supports. However, the shaft and bearing structure is assumed to be periodic which limits the generality of their analysis.

The scope of exact solutions is, therefore, severely limited.

ii) Approximate Methods: Included under this are a number of techniques. Applied to problems in vibrations, some of the popular ones are:

a) Rayleigh-Ritz method

b) Galerkin method

c) Transfer Matrix method

d) Finite Element method

Rayleigh-Ritz and Galerkin methods [13] require one to assume a series solution for the system. All basis functions in this series solution should satisfy the boundary conditions of the problem. The difficulty lies in choosing these basis functions to start with. As pointed

out in [7] the method calls for a certain degree of skill on the part of the user in its application.

Transfer Matrix Method (TMM): Pestel and Leckie [9] offer a first-rate treatment of the subject. Pilkey and Chang [10] have also applied the method to a wide variety of problems. Their text is in the nature of a handbook and contains exhaustive tabulation of transfer matrices for different systems.

In applying TMM one first needs the solution of the governing differential equation [9,10]. From this, one constructs the transfer matrix to relate state vectors on neighbouring stations. The state vector is transferred from one station to the next by 'field transfer matrices', briefly 'field matrices'. For points across which one or more state variables are discontinuous (like thin discs, in-span supports) state vector is transferred across this point by a 'point transfer matrix', briefly 'point matrix'. The state vector can thus be transferred across the entire rotor thereby relating state vectors at the rotor boundaries. Boundary conditions of the problem are then imposed and natural frequencies determined.

Although this is a powerful method, the limitation lies in the fact that many times one cannot find a general solution to the differential equation. Moreover, even when

this is possible, the expressions can be quite cumbersome and derivation of the transfer matrices a tedious task.

Finite Element Method (FEM): This is a powerful technique described in various texts [12,20] .

FEM does not suffer from the limitation pointed out for TMM above. Here generally a polynomial solution over the finite element is assumed. A matrix form of equations between state variables, valid for the finite element, is derived . Matrix equations for various elements are next assembled together.

This process of assembly leads to an increase in the order of matrices being handled. For a complicated system having many elements these matrices can become very large leading to large computer memory requirements. This drawback apart, FEM is a very powerful technique and is being widely used to solve a host of complex problems in a variety of fields in engineering.

1.2 Notes on the Transfer Finite Element Method (TFEM):

Gupta [4] has developed this elegant technique utilising ideas from both TMM and FEM. The method combines the advantages of both - reduced demand for computer memory without losing the polynomial solution advantage of FEM.

The matrix equations of the finite element obtained in the usual FEM are rearranged to yield transfer matrix. This relates state vectors at the neighbouring nodes as in TMM.

The TMM technique of multiplying these transfer matrices is used to obtain the overall transfer matrix [OT] between state vectors at the boundaries of the system. A determinant of residue is also obtained on similar lines by imposing boundary conditions. Hence 'assembly' for the entire system is different from the standard FEM and results in saving on computer memory.

Subramanya [11] has used this technique for the specialised topic of flexibility analysis of pipes.

CHAPTER 2

FORMULATION OF GOVERNING EQUATIONS

Earliest efforts at analysis of continuous systems of rotors made simplifying assumptions of neglecting rotary inertia, shear deformation, and gyroscopic effects. These simplifications lead to the classical Euler-Bernoulli formulations. However, results obtained from this formulation do not match known experimental values of natural frequencies and critical speeds, specially for higher modes and for short, stubby rotors. Lord Rayleigh and S.Timoshenko went into deeper analysis and showed that the effects of rotary inertia and shear deformations can be very significant in these cases. For rotors with large diameters and high rotational speeds, gyroscopic action of elements can also be significant.

Rotary inertia effect arises due to the fact that rotor elements not only move laterally in the plane of vibration but also rotate about an axis normal to this plane when the rotor bends. Again, shear deformation effect arises from the fact that shear forces on element faces cause deformation of the element and affect total slope. Total slope now is due to both bending moment and shear force. Both rotary inertia and shear are known [21] to decrease natural

frequencies vis-a-vis values obtained from classical Euler-Bernoulli theory.

Gyroscopic action occurs in rotors spinning about an axis passing through their geometric centre. Because of this rotation there is an angular momentum vector associated with each element. Transverse movement of the rotor causes a change in the angular momentum resulting in a gyroscopic couple being produced. As Rao [3] shows, this couple tends to straighten the shaft, i.e. it tends to realign the angular momentum vector with the centre line of the rotor. It therefore makes the rotor stiffer and increases values of natural frequency.

Critical speeds of a rotor are rotational speeds equal to the natural frequencies of transverse vibrations of the system. These are so called because all rotors, no matter how well balanced, have some amount of residual imbalance and this causes resonance when the rotor spins at a speed equal to its natural frequency. Whirling can become very large and even cause damage in such situations.

Equations are presented here for rotors taking into account rotary inertia, shear, and gyroscopic effects. Two approaches are presented — (i) two governing equations and, (ii) these combined into a single governing equation for the special case of rotor-segments with uniform cross-sectional properties. Some comments on these two approaches are presented

later in this chapter.

Equations are presented first in the dimensional form and then non-dimensionalised using characteristic values of length and time.

2.1 Basic Equations for Rotor:

These have been derived by various authors [1,2] and are being presented here for sake of completeness.

Rotor motion does not occur in one plane. Instead, the rotor spins about its axis as well as precesses about the bearing axis. It is thus necessary to consider the motion in two mutually perpendicular planes passing through the bearing axis. Coordinate system used is shown in Fig.2.1(a). Consider a thin section of length Δs on the rotor (referred to as 'eleme in this chapter but not to be confused with finite elements) in planes s-x and s-y.

Figure 2.1(c) shows the element in plane s-x. Figure 2.1(d) shows the details of slope of the element. Ψ_y is slope due to bending moment only while $\partial x/\partial s$ is total slope due to bending moment and shear.

From solid mechanics [13] we have the relations:

$$M_y = EI \frac{\partial \Psi_y}{\partial s} \qquad (2.1$$

$$S_x = k'GA \left(\frac{\partial x}{\partial s} - \Psi_y\right) \qquad (2.1$$

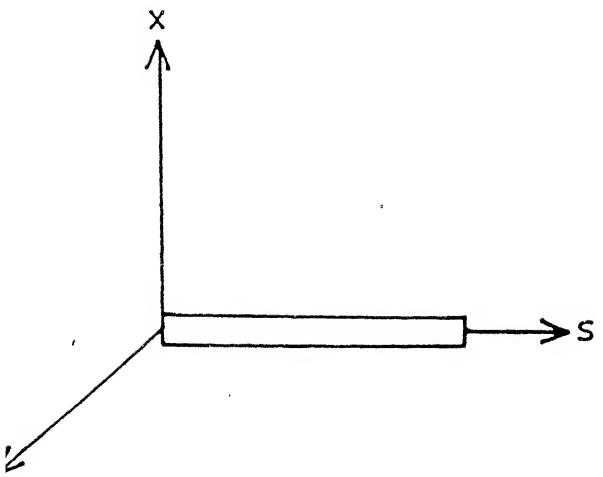

(a) Coordinate System

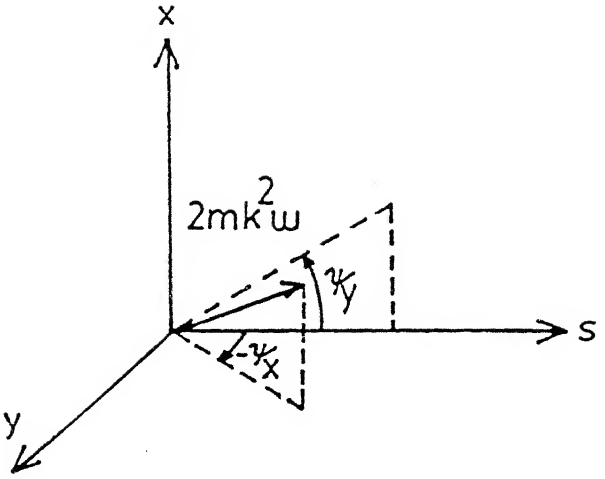

(b) Angles subtended by angular Momentum Vector

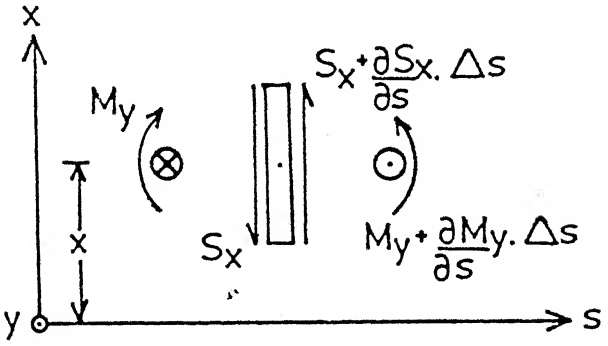

(c) Rotor section in plane s-x

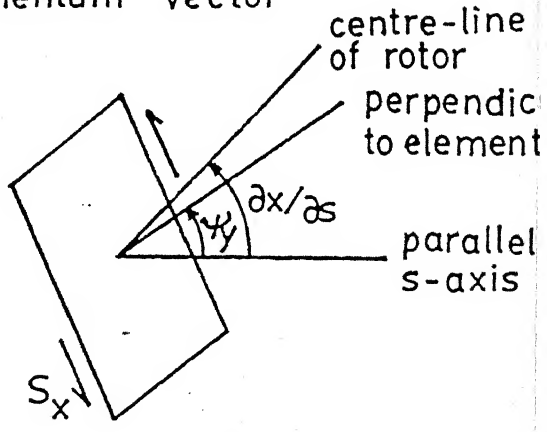

(d) Details of slope of rotor section in plane s-x

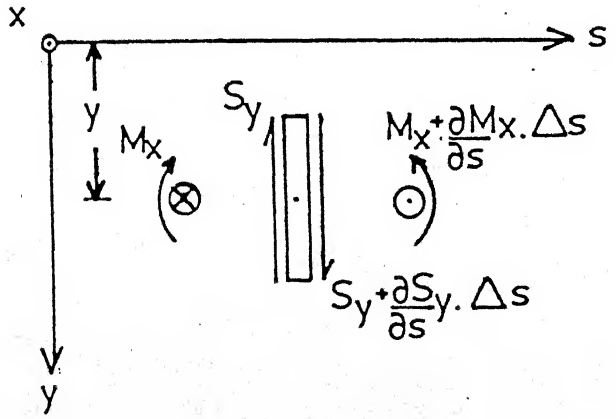

(e) Rotor section in plane s-y

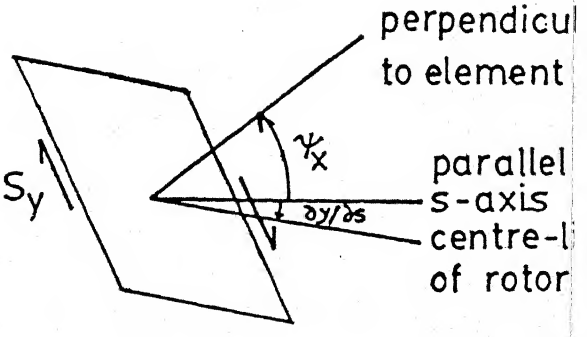

(f) Details of slope of rotor section in plane s-y

FIG 2.1 ROTOR SECTIONS

where k' is the appropriate form factor and is 0.9 for circular cross-section.

From force balance in x-direction

$$\frac{\partial S_x}{\partial s} = m \frac{\partial^2 x}{\partial t^2} \qquad (2.1.1$$

From moments balance about y-axis

$$M_y + \frac{\partial M_y}{\partial s}\Delta s - M_y + (S_x + \frac{\partial S_x}{\partial s}\Delta s)\frac{\Delta s}{2} + S_x \frac{\Delta s}{2}$$
$$= \frac{d}{dt}\left[mk^2 \frac{\partial \Psi_y}{\partial t} - 2mk^2 \omega \Psi_x\right]$$

or

$$\frac{\partial M_y}{\partial s} + S_x = mk^2 \frac{\partial^2 \Psi_y}{\partial t^2} - 2mk^2 \omega \frac{\partial \Psi_x}{\partial t} \qquad (2.1.1$$

First term on RHS of above equation is rotary inertia term while the second one is contribution from gyroscopic action of the elemental disc.

Similarly, for plane s-y, we have Fig.2.1(e), (f),

$$M_x = EI \frac{\partial \Psi_x}{\partial s} \qquad (2.1.2$$

$$S_y = k'GA\left(\frac{\partial y}{\partial s} + \Psi_x\right) \qquad (2.1.2$$

$$\frac{\partial S_y}{\partial s} = m \frac{\partial^2 y}{\partial t^2} \qquad (2.1.2$$

$$\frac{\partial M_x}{\partial s} - S_y = mk^2 \frac{\partial^2 \Psi_x}{\partial t^2} + 2mk^2 \omega \frac{\partial \Psi_y}{\partial t} \qquad (2.1.2)$$

2.2 Two Equation Approach:

Straightforward substitution of relations for M and S into the last two of equations (2.1.1) and (2.1.2) yield for plane s-x

$$\frac{\partial}{\partial s}\left[k'GA\left(\frac{\partial x}{\partial s} - \Psi_y\right)\right] = m \frac{\partial^2 x}{\partial t^2} \qquad (2.2.1)$$

$$\frac{\partial}{\partial s}\left(EI \frac{\partial \Psi_y}{\partial s}\right) + k'GA\left(\frac{\partial x}{\partial s} - \Psi_y\right) = mk^2 \frac{\partial^2 \Psi_y}{\partial t^2} - 2mk^2 \omega \frac{\partial \Psi_x}{\partial t}$$

and for plane s-y

$$\frac{\partial}{\partial s}\left[k'GA\left(\frac{\partial y}{\partial s} + \Psi_x\right)\right] = m \frac{\partial^2 y}{\partial t^2} \qquad (2.2.2)$$

$$\frac{\partial}{\partial s}\left(EI \frac{\partial \Psi_x}{\partial s}\right) - k'GA\left(\frac{\partial y}{\partial s} + \Psi_x\right) = mk^2 \frac{\partial^2 \Psi_x}{\partial t^2} + 2mk^2 \omega \frac{\partial \Psi_y}{\partial t}$$

Multiplying equations (2.2.2) by $i = \sqrt{-1}$ and defining complex displacement as $z = x + iy$, complex slope as $\Psi = \Psi_y - i\Psi_x$, one can combine the above equations to get:

$$m\ddot{z} - \frac{\partial}{\partial s}\left[k'GA(z' - \Psi)\right] = 0 \qquad (2.2.3)$$

$$\frac{\partial}{\partial s}\left(EI\,\Psi'\right) + k'GA(z' - \Psi) - mk^2 \ddot{\Psi} + 2imk^2 \omega \dot{\Psi} = 0$$

where primes denote derivatives w.r.t. s and dot w.r.t. time, t.

Equations (2.2.3) are the coupled governing differential equations for a rotor.

In order to obtain non-dimensional form of the above equation, for the present work the special case of constant cross-sectional properties is considered. The two equation approach has been used only for comparison of results with one-equation approach for this specific case. As pointed out earlier, other problems have been solved using the single governing equation approach.

For constant cross-sectional properties, non-dimensionalised equations are (See Appendix A)

$$\frac{\partial}{\partial S}\,(Z' - \Psi) - Mc.Re^2.\ddot{Z} = 0$$

$$\frac{\partial}{\partial S}\,\Psi' + \frac{1}{Mc.Re^2}\,(Z' - \Psi) - Re^2\,(\ddot{\Psi} - 2i\Omega\,\dot{\Psi}) = 0 \qquad (2.2.$$

2.3 Single Equation Approach:

Equations (2.2.3) above can be combined to yield a single fourth order governing differential equation for the special case of constant cross-sectional properties.

Assuming that k'GA is a constant, we obtain from relations (2.1.1b,c) the expressions

$$\frac{\partial \Psi_y}{\partial s} = \frac{\partial^2 x}{\partial s^2} - \frac{m}{k'GA} \frac{\partial^2 x}{\partial t^2}$$

$$\frac{\partial^3 \Psi_y}{\partial s^3} = \frac{\partial^4 x}{\partial s^4} - \frac{m}{k'GA} \frac{\partial^4 x}{\partial s^2 \partial t^2} \qquad (2.3.1$$

and from (2.1.2b,c) the expressions:

$$\frac{\partial \Psi_x}{\partial s} = \frac{m}{k'GA} \frac{\partial^2 y}{\partial t^2} - \frac{\partial^2 y}{\partial s^2}$$

$$\frac{\partial^3 \Psi_x}{\partial s^3} = \frac{m}{k'GA} \frac{\partial^4 y}{\partial s^2 \partial t^2} - \frac{\partial^4 y}{\partial s^4} \qquad (2.3$$

Assuming again that EI is constant, differentiating equations (2.1.1d) and (2.1.2d) once w.r.t. s and using expressions (2.3.1) and (2.3.2) we obtain equations for the two planes. These can be combined as for the two-equation approach to yield the single governing equation in z:

$$\frac{EI}{m} z^{IV} - k^2 \left(1 + \frac{E}{k'G}\right) \ddot{z}'' + 2i\omega k^2 \dot{z}'' + \ddot{z} + \frac{mk^2}{k'GA} \ddot{z}'' - 2i\omega \frac{mk^2}{k'GA} \dot{z} = 0 \qquad (2.3$$

Equation (2.3.3) (as also equations (2.2.4)) takes into account rotary inertia, shear effects, and gyroscopic effects.

Timoshenko beam and Euler beam equations are special cases of equation (2.3.3). The former requires us to neglect gyroscopic effects and the equation can be established by taking $\Omega = 0$ in this equation. Euler beam formulation neglects all the above mentioned effects and hence the equation can be obtained from equation (2.3.3) by retaining only the z^{IV} and $\ddot{z}$ terms.

In the non-dimensional form equation (2.3.3) is (Appendix A):

$$z^{IV} - Re^2 (1+Mc)\, \ddot{Z}'' + 2i\Omega.Re^2\, \dot{Z}'' + Mc.Re^4\, \ddot{Z}'' + \ddot{Z} - 2i\,\Omega.Mc.Re^4\, \dot{\ddot{Z}} = 0 \qquad (2.3.4)$$

2.4 Non-dimensionalised Equations for Rotor with Discrete Changes in Cross-sectional Area

Consider the rotor shown in fig.2.2 below:

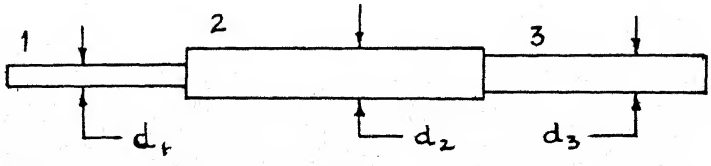

Fig.2.2 : Rotor with discrete changes in cross-sectional area.

The three segments have cross-sectional areas A_1, A_2 and A_3 with corresponding diameters d_1, d_2 and d_3. E, G and k' are considered same for all sections.

Equation (2.3.3) is applicable to a shaft section with uniform cross sectional properties. This equation is therefore applicable to sections 1,2 and 3 of the shaft with suitable values of cross-sectional variables. Thus for jth section

$$E\left[\frac{I}{m}\right]_j \frac{\partial^4 z}{\partial s^4} - k_j^2\left(1 + \frac{E}{k'G}\right)\frac{\partial^4 z}{\partial s^2 \partial t^2} + 2i\omega k_j^2 \frac{\partial^3 z}{\partial s^2 \partial t} + \frac{\partial^2 z}{\partial t^2} + \left[\frac{mk^2}{A}\right]_j \frac{1}{k'G} \cdot \frac{\partial^4 z}{\partial t^4} - 2i\omega\left[\frac{mk^2}{A}\right]_j \frac{1}{k'G} \frac{\partial^3 z}{\partial t^3} = 0$$

(2.4.1

To non-dimensionalise this equation, one can use overall shaft length L, and characteristic time $T_* = (mL^4/EI)^{1/2}$ based on characteristic values of m and I of any section. Denoting these characteristic values by non-subscripted quantities, one has from equation (2.4.1):

$$\frac{EI}{m} \cdot \frac{m}{m_j} \cdot \frac{I_j}{I} \cdot \frac{1}{L^3} z^{IV} - k^2\left[\left(1 + \frac{E}{k'G}\right)\frac{1}{LT_*^2}\ddot{z}'' - 2\frac{\Omega}{T_*}\frac{1}{LT_*}\dot{z}''\right] \cdot \frac{k_j^2}{k^2}$$

$$+ \frac{L}{T_*^2} \ddot{Z} + \left[\frac{mk^2}{A}\right]_j \frac{1}{k'G} \frac{L}{T_*^4} \dddot{Z} - 2i \frac{\Omega}{T_*} \cdot \left[\frac{mk^2}{A}\right]_j \cdot$$

$$\frac{1}{k'G} \cdot \frac{L}{T_*^3} \ddot{Z} = 0$$

Now,

$$\frac{EI}{mL^3} = \frac{L}{T_*^2} \quad , \quad \frac{(I/m)_j}{I/m} = \left(\frac{d_i}{d}\right)^2 \quad \text{with} \quad \rho_j = \rho$$

and

$$\frac{1}{T_*^2} \cdot \left[\frac{mk^2}{A}\right]_j \frac{1}{k'G} = \frac{E}{k'G} \cdot \frac{k^4}{L^4} \cdot \frac{k_j^2}{k^2} \cdot$$

Also, $k_j/k \equiv d_j/d$.

Denoting d_j/d by Rd_j (relative diameter of section j with respect to characteristic diameter, d), we have:

$$Rd_j^2 . Z^{IV} - Re^2 . Rd_j^2 \left[(1 + Mc) \ddot{Z}'' - 2i \Omega \dot{Z}''\right]$$
$$+ \ddot{Z} + Mc . Re^4 . Rd_j^2 \dddot{Z} - 2i \Omega . Mc . Re^4 . Rd_j^2 \ddot{Z} = 0$$

(2.4.2)

where Re = k/L is based on characteristic k.

The above equation is, for the present work, the most general form of the governing differential equation for transverse vibrations of a rotor. Putting $Rd_j = 1.0$ for all sections

would yield, the equation for a uniform rotor (ref. equation 2.3.4).

CHAPTER 3

FINITE ELEMENT FORMULATIONS

In the course of the present work, it was observed that using two coupled differential equations for obtaining natural frequencies and critical speeds leads to problems of poor convergence. This happens because equations become ill-conditioned. Reduced numerical integration using Gaussian quadrature has to be carried out to overcome this problem [19,20]. It may mentioned that if one is interested in situations where cross-sectional area of the shaft varies continuously along the shaft length, one shall necessarily have to use a two-equation approach for it does not seem possible to combine the two equations to yield a single governing differential equation for such a case. However, if instead one is interested in situations where shaft section changes are discrete with cross-sectional area being constant for a given segment, one can use a single governing equation approach.

The two equation approach is also the more useful one when one is faced with situations where both ends of the beam/rotor are built-in (or fixed). This is so because by using this approach one can satisfy both the geometrical boundary conditions exactly.

Details of the finite element formulation have been provided here with reference to the single governing equation of fourth order. Formulation for the two-equation approach is presented in Appendix B.

From the previous chapter it is seen that for a rotor equation (2.4.2) is more general and differs from equation (2.3.4) in only some constant factors to account for differences in cross-sectional properties. Equation (2.4.2) is therefore used as the basic one for deriving finite element formulations here. This equation is presented again, with minor modifications, for ease of reference:

$$C_1 z^{IV} - C_2 \left[(1 + Mc)\, \ddot{z}'' - 2i\,\Omega\, \dot{z}'' \right] + \ddot{z} + C_3 \cdot \ddot{z} - 2i\,\Omega \cdot C_3 \cdot \dot{z} = 0 \qquad (3.1)$$

where

$$C_1 = Rd_j^2,\ C_2 = (Re * Rd_j)^2,\ C_3 = Mc.Re^4.Rd_j^2 .$$

Consider the rotor divided into number of finite elements, as in figure 3.1

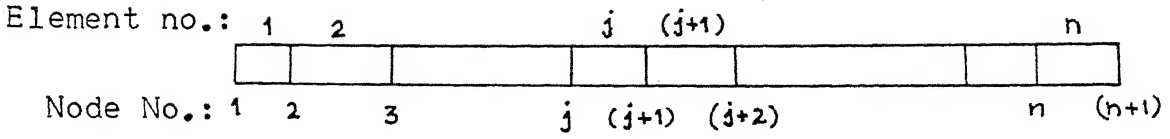

(a)

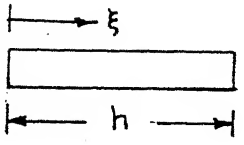

(b)

Fig.3.1:(a) Rotor divided into finite elements
(b) Typical finite element

A typical element is also shown in the figure. Local coordinate along the length is ξ and element length is h. In non-dimensionalised form, we have $\eta = \xi/L$ and $H = h/L$.

The governing equation applicable to the element is then:

$$C_1 \frac{\partial^4 Z}{\partial \eta^4} - C_2\left[(1 + Mc) \frac{\partial^4 Z}{\partial \eta^2 \partial T^2} - 2i\Omega \frac{\partial^3 Z}{\partial \eta^2 \partial T}\right] + \frac{\partial^2 Z}{\partial T^2}$$

$$+ C_3 \frac{\partial^4 Z}{\partial T^4} - 2i\Omega C_3 \cdot \frac{\partial^3 Z}{\partial T^3} = 0 \qquad (3.2)$$

where

$$Z = Z(\eta, T) .$$

Assume a polynomial solution over the element,

$$Z^{(e)}(\eta, T) = \lfloor N_1 \; N_2 \; \ldots \; N_r \rfloor \lfloor Z_1 \; Z_2 \; \ldots \; Z_r \rfloor^T$$

or

$$Z^{(e)} = \lfloor N \rfloor \{Z\}^{(ne)} \qquad (3.3)$$

where N_i are shape functions dependent only on η and Z_i are variables at nodes of element and are functions of time only. Since this is an assumed solution, it will not satisfy the governing equation exactly. Substitution of expression (3.3) in equation (3.2) leaves a residue over the element, $Res^{(e)}$,

$$Res^{(e)} = C_1 \frac{\partial^4 Z^{(e)}}{\partial \eta^4} - C_2 \left[(1 + Mc) \frac{\partial^4 Z^{(e)}}{\partial \eta^2 \partial T^2} - 2i\Omega \frac{\partial^3 Z^{(e)}}{\partial \eta^2 \partial T} \right] + \frac{\partial^2 Z^{(e)}}{\partial T^2} + C_3 \frac{\partial^4 Z^{(e)}}{\partial T^4} - 2i\Omega C_3 \cdot \frac{\partial^3 Z^{(e)}}{\partial T^3} \qquad (3.4)$$

This residue needs to be minimised. Different techniques are available for this. Here the most successful Galerkin method [16] has been used. Thus one gets

$$\int_0^H N_i \cdot Res^{(e)} \cdot d\eta = 0$$

$$i = 1, 2, \ldots, r \qquad (3.5)$$

Equation (3.5) is integrated by parts, till the derivatives are reduced to the lowest order possible. Using expression (3.3) this becomes:

$$C_1 \int_o^H \{N''\}\lfloor N''\rfloor \, d\eta\{Z\}^{(ne)} + C_2(1+Mc) \int_o^H \{N'\}\lfloor N'\rfloor \, d\eta\{\dot{Z}\}^{(ne)}$$

$$- C_2 \cdot 2i\Omega \int_o^H \{N'\}\lfloor N'\rfloor \, d\eta\{\dot{Z}\}^{(ne)}$$

$$+ \int_o^H \{N\}\lfloor N\rfloor \, d\eta\{\ddot{Z}\}^{(ne)} + C_3 \int_o^H \{N\}\lfloor N\rfloor d\eta\{\dddot{Z}\}^{(ne)}$$

$$- 2i\Omega C_3 \int_o^H \{N\}\lfloor N\rfloor \, d\eta\{\ddot{Z}\}^{(ne)}$$

$$= C_1\{N'\}\frac{\partial^2 Z(e)}{\partial\eta^2}\Big|_o^H - C_1\{N\}\frac{\partial^3 Z(e)}{\partial\eta^3}\Big|_o^H + C_2(1+Mc)\{N\}\frac{\partial^3 Z(e)}{\partial\eta\partial T^2}\Big|$$

$$- 2i\Omega C_2 N \frac{\partial^2 Z(e)}{\partial\eta\partial T}\Big|_o^H \qquad (3.6)$$

No comment has so far been made on the number of terms in the polynomial approximation (3.3) and on the nature of shape functions N_i. Various finite element models using different shape functions have been used in the literature for the dynamic analysis of Timoshenko beams. Thomas and Abbas [14] have given a comparison of different models used by various investigators and have also presented a better finite element model. Earlier models, they have claimed, did not represent the Timoshenko beam accurately because all boundary conditions could not be applied satisfactorily. Their model is an element with eight degrees of freedom requiring eight nodal coordinates. They have

assumed cubic polynomial approximations for total deflection and bending slope of the element. No justification has been given for this choice of higher order element.

Gupta [4] and Singh and Singh [15] have used a rational approach of Huebner [16] for deciding the number of terms in the interpolating polynomial. In both cases finite element equations are systematically and logically derived from the governing differential equations of the system using the Galerkin method and the order of the approximating polynomial is obtained from the conditions of compatibility and completeness as outlined by Huebner [16] . This approach is followed here.

The finite element equations (3.6) have been derived using the Galerkin method from the governing differential equation (2.4.2). The highest order of the derivative appearing under the integral sign in equation (3.6) is two which requires a compatibility of Z and first derivative. The highest order derivative in the same equations is three and hence completeness of Z and derivatives upto third order is required. Therefore, the approximating polynomial needs to be of third order. Thus the finite element model for this problem can be a two noded element with Z and Z' as degrees of freedom at each node. Shape functions satisfying the above requirements of compatibility and completeness are [12] :

$$N = \left[\, 1 - \frac{3\eta^2}{H^2} + \frac{2\eta^3}{H^3} \quad \eta - \frac{2\eta^2}{H} + \frac{\eta^3}{H^2} \quad \frac{3\eta^2}{H^2} - \frac{2\eta^3}{H^3} \quad - \frac{\eta^2}{H} + \frac{\eta^3}{H^2} \,\right] \tag{3.7}$$

and nodal variables are:

$$\{Z\}^{(ne)} = [\, Z_1 \quad Z_1' \quad Z_2 \quad Z_2' \,]^T \tag{3.8}$$

Using expression (3.7), various matrices of equation(3.6) can be evaluated and this equation written as

$$C_1 [K] \{Z\}^{(ne)} + C_2 (1 + Mc) [MB] \{\ddot{Z}\}^{(ne)} - C_2 \, 2i \, \Omega [MB] \{\dot{Z}\}^{(ne)} + [M] \{\ddot{Z}\}^{(ne)} + C_3 [M] \{\dddot{Z}\}^{(ne)} - 2i \Omega C_3 [M] \{\ddot{Z}\}^{(ne)}$$

$$= \left\{ \begin{array}{l} \left(C_1 \frac{d^3 Z^{(e)}}{d\eta^3} - C_2 \left((1+Mc) \frac{3 Z^{(e)}}{T^2} - 2i \frac{\partial^2 Z^{(e)}}{\partial \eta \partial T} \right) \right) \Big|_{\eta = 0} \\ - C_1 \frac{d^2 Z^{(e)}}{d\eta^2} \Big|_{\eta = 0} \\ - \left(C_1 \frac{d^3 Z^{(e)}}{d\eta^3} - C_2 \left((1+Mc) \frac{\partial^3 Z^{(e)}}{\partial \eta \partial T^2} - 2i \frac{\partial^2 Z^{(e)}}{\partial \eta \partial T} \right) \right) \Big|_{\eta =} \\ C_1 \frac{d^2 Z^{(e)}}{d\eta^2} \Big|_{\eta = H} \end{array} \right. \tag{3.9}$$

where

$$[K] = \int_0^H \{N''\} \lfloor N'' \rfloor \, d\eta$$

$$[M] = \int_0^H \{N\} \lfloor N \rfloor \, d\eta$$

$$[MB] = \int_0^H \{N'\} \lfloor N' \rfloor \, d\eta$$

are square matrices of order 4x4. The elements of these matrices with $\lfloor N \rfloor$ as in expression (3.7) are given in Appendix C.

We can expect the system to behave periodically in time. Thus one can take the solution in the form

$$\{Z\}^{(ne)} = \{\bar{Z}\}^{(ne)} \cdot e^{i\lambda T} \tag{3.10}$$

where $\bar{Z}$ are magnitudes and λ is the frequency (non-dimensional in this case since T is non-dimensional).

Using expression (3.10), one can rewrite equations (3.9) as (dropping superscript (e) on Z for convenience) :

$$\left[C_1[K] - C_2((1+Mc)\cdot\lambda^2 - 2\Omega\lambda)[MB] + (C_3\lambda^4 - C_3\cdot 2\lambda^3\Omega - \lambda^2)[M]\right]\{Z\}^{(ne)}$$

$$= \left\{ \begin{array}{l} (C_1 \dfrac{d^3Z}{d\eta^3} + C_2(\lambda^2(1+Mc) - 2\Omega\lambda)\dfrac{dZ}{d\eta}\Big|_{\eta=0} \\ - C_1 \dfrac{d^2Z}{d\eta^2}\Big|_{\eta=0} \\ - (C_1 \dfrac{d^3Z}{d\eta^3} + C_2(\lambda^2(1+Mc) - 2\Omega\lambda)\dfrac{dZ}{d\eta})\Big|_{\eta=H} \\ C_2 \dfrac{d^2Z}{d\eta^2}\Big|_{\eta=H} \end{array} \right\} \tag{3.11}$$

Noting that $\eta = 0$ and $\eta = H$ correspond respectively to nodes 1 and 2 of an element, one can rewrite equation (3.11) more briefly as:

$$\left[P[K] + Q[MB] + R[M] \right] \begin{Bmatrix} Z_1 \\ Z_1' \\ Z_2 \\ Z_2' \end{Bmatrix} = \begin{Bmatrix} -V_1 \\ -M_1 \\ V_2 \\ M_2 \end{Bmatrix} \qquad (3.12)$$

where

$$P = C_1$$

$$Q = -C_2 \left((1 + Mc)\lambda^2 - 2\Omega\lambda \right)$$

$$R = C_3\lambda^4 - C_3 \cdot 2\Omega\lambda^3 - \lambda^2$$

$$V_j = -\left(C_1 \frac{d^3Z}{d\eta^3} + C_2 \left(\lambda^2 (1 + Mc) - 2\Omega\lambda \right) \frac{dZ}{d\eta} \right) \Bigg|_j$$

$$M_j = C_1 \frac{d^2Z}{d\eta^2} \Bigg|_j$$

The above are the finite element matrix equations for a rotor element taking into account rotary inertia, shear deformation and gyroscopic effects.

CHAPTER 4

F.E. TRANSFER MATRICES AND METHOD OF SOLUTION

4.1 Finite Element Transfer Matrices

The assembled matrix $\left[P[K] + Q[MB] + R[M]\right]$ of equations (3.15) is a square 4x4 matrix. From equation (3.15) one sees that this assembled matrix relates nodal variables Z and Z' to the forces V and moments M at the nodes. To obtain the transfer matrix which provides a relation between variables at nodes 1 and 2, the equations (3.12) are rearranged. To achieve this, the equation (3.12) are partitioned into submatrices as follows:

$$\begin{bmatrix} [A] & [B] \\ [C] & [D] \end{bmatrix} \begin{Bmatrix} \{W\}_1 \\ \{W\}_2 \end{Bmatrix} = \begin{Bmatrix} -\{F\}_1 \\ \{F\}_2 \end{Bmatrix} \qquad (4.1.1)$$

where

$$\{W\}_j = \begin{Bmatrix} Z_j \\ Z'_j \end{Bmatrix} \text{ and } \{F\}_j = \begin{Bmatrix} V_j \\ M_j \end{Bmatrix}; \quad j = 1,2 ,$$

then one has

$$\begin{aligned} [A]\ \{W\}_1 + [B]\{W\}_2 &= -\{F\}_1 \\ [C]\ \{W\}_1 + [D]\{W\}_2 &= \{F\}_2 \end{aligned} \qquad (4.1.2)$$

From the first of equations (4.1.2) one gets

$$\{W\}_2 = -[B]^{-1}[A]\{W\}_1 - [B]^{-1}\{F\}_1$$

Usingthis, from the second equation of (4.1.2) one gets

$$\{F\}_2 = [C] - [D][B]^{-1}[A]\{W\}_1 - [D][B]^{-1}\{F\}_1$$

The above two equations are put together to yield the following transfer matrix equation:

$$\begin{Bmatrix}\{W\}\\ \{F\}\end{Bmatrix}_2 = \begin{bmatrix} -[B]^{-1}[A] & -[B]^{-1} \\ [C]-[D][B]^{-1}[A] & -[D][B]^{-1}\end{bmatrix} \begin{Bmatrix}\{W\}\\ \{F\}\end{Bmatrix}_1 \qquad (4.1.3)$$

Writing this more concisely and for the general case of the jth element having nodes j and (j+1),

$$\{SV\}_{j+1} = [T]_j \{SV\}_j \qquad (4.1.4)$$

where $\{SV\}_j$ is the state vector at node j and $[T]_j$ is the field transfer matrix for the (finite) element j.

METHOD OF SOLUTION

4.2 Rotor without In-span Supports

Consider the rotor divided into n elements (Fig.3.1 , Page 22). Recursive relationship (4.1.4) yields:

$$\{SV\}_{n+1} = [T]_n \; [T]_{n-1} \; \cdots \; [T]_1 \; \{SV\}_1$$

or

$$\{SV\}_{n+1} = [OT] \; \{SV\}_1 \qquad (4.2.1)$$

where [OT] is the overall transfer matrix between state-vectors at nodes 1 and (n+1). Boundary conditions at these nodes can then be used to obtain a determinant of order two which goes to zero for natural frequency values of λ. For critical speeds, forward whirl requires Ω equal to λ while backward whirl requires Ω equal to $-\lambda$.

4.3 Rotor with In-Span Supports

In-span supports considered are all of the 'simple' kind allowing continuity of slope and bending moment while imposing the condition that deflection is zero. A clamped in-span support would be equivalent to having the shafts isolated from each other for the case of transverse vibrations.

A simple in-span support introduces a shear discontinuity. It is assumed that other components of state vector {SV} remain continuous across such a support. It may be mentioned that this assumption implies an approximation when considering shear effects on the shafts if a single governing equation is used because actually slope

due to bending moment alone would remain continuous. Since there is a shear discontinuity, the slope due to shear effects and consequently the total slope will change across the support. However, since this effect is usually small it does not appear to be an unreasonable approximation. Difficulties with using a two equation approach where this distinction could be maintained have been pointed out earlier.

Introduction of a shear discontinuity necessitates the derivation of a 'point transfer matrix', briefly point matrix, for transferring state vector variables from one side of the support to the other.

Two methods are available for handling such situations. Pestel and Leckie [9] follow a technique involving elimination of unknownsat different in-span supports and they reduce the size of matrices being handled by appropriate manipulations. Pilkey and Chang [10], on the other hand, derive point matrices of same order as field matrices using a condition from the station to the right of the in-span support. The latter is the more elegant method in terms of programming the computer. Subramanya [11] has used it in conjunction with transfer FEM. The same technique is used here.

Two cases are handled:

(a) in-span support with simple support on its right (to handle shafts with both extremities on simple supports), and

(b) in-span support with free end on its right (to take care of cases with overhang)

4.3.1 In-span support with Simple Support on its Right

The specific case of Figure 4.1(a) is considered with two in-span supports and simple supports at shaft extremeties. Generalising to a case of a n in-span supports will be a simple matter.

This shaft has three spans, each simply-supported on both ends. $[T]_{sj}$ is the field transfer matrix for span j while $\{SV\}_{pj}$ is the state vector at support point j.

Since force V is discontinuous across in-span support, superscripts L and R are used on V to denote force just to the left and right respectively of support j. Other state variables being continuous across the support, no superscript is used on them.

To obtain point matrix for support 2, transfer matrix relation for span 2 is used as follows:

$$\begin{Bmatrix} Z \\ Z' \\ V^L \\ M \end{Bmatrix}_{p3} = \begin{bmatrix} T_{11} & T_{12} & T_{13} & T_{14} \\ \cdot & \cdot & \cdot & \cdot \\ \cdot & \cdot & \cdot & \cdot \\ T_{41} & \cdot & \cdot & T_{44} \end{bmatrix}_{s2} \cdot \begin{Bmatrix} Z \\ Z' \\ V^R \\ M \end{Bmatrix}_{p2} \qquad (4.3.1)$$

Since $Z_{p3} = 0$ one gets

$$V^R_{p2} = - \frac{T_{11}}{T_{13}} Z_{p2} - \frac{T_{12}}{T_{13}} Z'_{p2} - \frac{T_{14}}{T_{13}} M_{p2}$$

where T_{ij} are from T_{s2}.

Using the above expression, state vectors on the two sides of support 2 can be related as

$$\begin{Bmatrix} Z \\ Z' \\ V^R \\ M \end{Bmatrix}_{p2} = \begin{bmatrix} 1 & 0 & 0 & 0 \\ 0 & 1 & 0 & 0 \\ -\frac{T_{11}}{T_{13}} & -\frac{T_{12}}{T_{13}} & 0 & -\frac{T_{14}}{T_{13}} \\ 0 & 0 & 0 & 1 \end{bmatrix}_2 \begin{Bmatrix} Z \\ Z' \\ V^L \\ M \end{Bmatrix}_{p2} \qquad (4.3.2)$$

or

$$\{SV\}^R_{p2} = [P]_2 \{SV\}^L_{p2}$$

where $[P]_2$ is point matrix for support 2.

Point matrix for support 3 can be obtained in a similar fashion using $[T]_{s3}$. The overall relationship then becomes:

$$\{SV\}_{p4} = [T]_{s3} [P]_3 [T]_{s2} [P]_2 [T]_{s1} \{SV\}_{p1} \qquad (4.3.3)$$

or $\{SV\}_{p4} = [OT] \{SV\}_{p1}$

where [OT] is the overall transfer matrix.

To get the determinant for finding the natural frequencies, along with unused boundary conditions of the system one is required to use the unutilized condition of an in-span support. For the present case, boundary condition $Z_{p4} = 0$ has been utilised in obtaining $[P]_3$. From equation (4.3.3), using the remaining boundary conditions, one gets:

$$OT_{42} \cdot Z'_{p1} + OT_{43} \cdot V_{p1} = 0 \qquad (4.3.4a)$$

while from transfer matrix relationsfor span 1 and making use of the unutilized condition $Z_{p2} = 0$;

$$T_{12}\, Z'_{p1} + T_{13}\, V_{p1} = 0 \qquad (4.3.4b)$$

where T_{12}, T_{13} are from $[T]_{s1}$.

Putting equations (4.3.4) together one obtains the determinant to be satisfied as:

$$\begin{vmatrix} T_{12} & T_{13} \\ OT_{42} & OT_{43} \end{vmatrix} = 0 \qquad (4.3.5)$$

4.3.2 In-span support with Free End on its Right

Consider the specific case of Figure 4.1(b). As before there are two in-span supports but point 4 is free unlike the previous case of section 4.3.1. Point matrix for

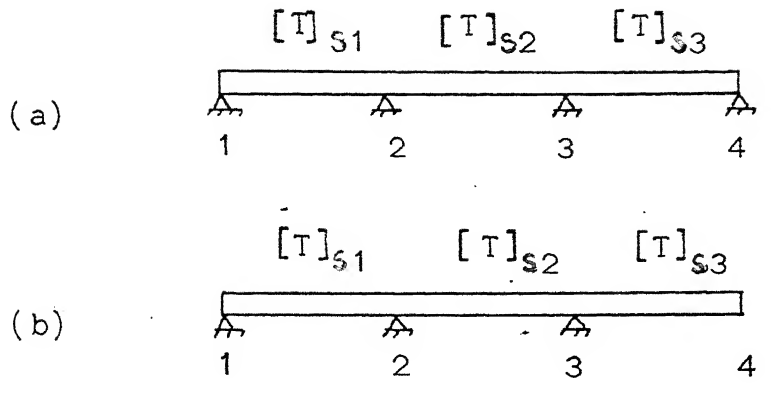

Figure 4.1 : Multi-span rotors (a) both ends supported (b) with overhang

support 2 is derived as in the previous section. For support 3, however, one needs to use a different condition, viz. $M_{p4} = 0$ to derive the point matrix.

Along lines similar to those followed in the previous section, one has

$$\{SV\}_{p4} = [T]_{s3} \{SV\}^{R}_{p3}$$

from which, with $M_{p4} = 0$, one gets

$$V^{R}_{p3} = - \frac{T_{41}}{T_{43}} Z_{p3} - \frac{T_{42}}{T_{43}} Z'_{p3} - \frac{T_{44}}{T_{43}} M_{p3}$$

Point matrix $[P]_3$ is hence:

$$[P]_3 = \begin{bmatrix} 1 & 0 & 0 & 0 \\ 0 & 1 & 0 & 0 \\ -\frac{T_{41}}{T_{43}} & -\frac{T_{42}}{T_{43}} & 0 & -\frac{T_{44}}{T_{43}} \\ 0 & 0 & 0 & 1 \end{bmatrix} \qquad (4.3.6)$$

Rest of the procedure is similar to that outlined in the previous section 4.3.1.

CHAPTER 5

RESULTS AND DISCUSSIONS

FORTRAN programs have been developed for determination of natural frequencies and critical speeds using the one governing equation approach for a variety of cases. The two equation approach has also been used for the case of a uniform rotor.

Results are presented in Table 1 through to Table 7 and Figure 5.1 to Figure 5.2. The discussion that follows is with reference to particular tables and figures. Exact results where presented mean results obtained from a closed-form formulation.

In the presentation of these results two values of factor Re (= k/L) have been used frequently. Small Re value (denoted by Re_S in some tables) of 0.0125 corresponds to a rotor with diameter being 1/20 of rotor length ('slender' rotor) while large Re (denoted as Re_L) of 0.05 corresponds to a 'stubby' rotor with diameter being 1/5 of the total rotor length. For a steel shaft of circular cross section, material constant Mc (= E/k'G) is 2.9 and this is the value used throughout.

Table 1: Critical speeds for simple-simple, cantilever and fixed-fixed rotors are shown for various number of elements. Exact critical speeds available for simple-simple rotor [1] are also shown. Study of this table shows that one can safely take 6 elements. For simple-simple case with 6 elements error in the first mode is 0.01% and in the fourth mode is 1.03%.

Some general trends that can be observed are:

i) results converge from above, i.e. values obtained are larger than the exact values, and

ii) error is more in higher modes.

These trends are usually observed in vibration problems solved using finite element method.

Figures 5.1 and 5.2: These show the natural frequencies for different modes as functions of rotor speed, Ω. Figure 5.1 shows this for a uniform rotor for which shear deformation effects have been ignored. Natural frequency is seen to increase with rotor speed. Numerical difficulties did not allow determination of λ for rotor speeds more than 600 for the case considered (Re = 0.05). From a practical point of view, Ω = 600 is a very high speed, being about sixty times the first critical speed.

Figure 5.2 shows the natural frequency versus rotor speed plot for a simple-simple rotor with Re = 0.05 with shear

effect included. Shear effect, it is seen, tends to reduce natural frequencies and also makes the curves flatten out at very high rotor speeds.

In both cases, results are seen to match very well with those obtained from exact formulation [1]. Hence the present technique can be used for quick and accurate determination of variation of natural frequencies for all types of rotor systems as a function of rotor speeds.

Table 2: Results in this case are from two governing equations approach. With exact integration, ill-conditioning was observed. Reduced integration was used to over come this problem [4,19]. Even with this, convergence is observed to be slow. For the simple-simple supports case, comparison with exact results shows that critical speed values converge to an answer that is less than the exact.

Table 3: This gives results for three different rotors using one and two governing equations approaches for small and large values of Re. Problem of ill-conditioning of equations is seen to be serious for small Re values for which answers are seen to be higher than those obtained from a single equation approach. For large Re, however, the opposite is seen to hold true.

Due to the erractic behaviour of results due to ill-conditioning, this two governing equations approach has not been pursued further.

Table 4: Results for three different cases of end supports are presented for both small and large Re values. For small Re, results are seen to be very close to the natural frequency values of an Euler beam while for large Re, these are significantly lower. This is to be expected since accounting for Timoshenko effects affects natural frequencies significantly for thick beams/rotors. The effect of gyroscopic action of rotor elements is shown by a comparison of natural frequency/ critical speed values of Timoshenko beams and rotors. As seen from the table, gyroscopic effect tends to increase the natural frequency of the system and is quite significant for large Re and higher modes. This is to be expected since firstly large Re implies a thicker rotor, and secondly higher modes imply larger curvature of shaft. Both imply large gyroscopic moment and hence increased effect of the gyroscopic action.

Table 5: Some cases of multi-span beams/rotors with different sets of end-supports have been considered here. The table also shows schematically the various cases considered With reference to these figures, the fractional numbers (just above the shaft line) give the non-dimensional span lengths whi

the whole numbers (just below the shaft line) give the number of elements used for the span. To check the validity of the method employed to handle such problems, results for Euler beams from the transfer FEM are compared with exact results [18] and are seen to be in good agreement. It may be mentioned that the 'exact' values quoted for the simple-simple case have been obtained from a graph in [18] while for the other cases these have been obtained from tables in [18] . Exact values [18] for the simple-simple case are therefore relatively inaccurate.

Table 6: For a double-span beam, changing position of the in-span support changes the critical speeds of a rotor and this fact can have useful applications in systems where the designer has the freedom to select the position of this support. Table 6 gives the variation in critical speeds for some different positions of the in-span support for uniform rotors. Different sets of end-supports have been considered. These results were seen to follow patterns similar to those obtained by Gorman [18] for Euler beams.

For the uniform rotors considered, two observations can be made. Firstly, it is seen that critical speeds vary considerably as in-span support position is varied. Secondly, this variation is such that the difference between the first two critical speeds also varies. This difference is seen to be

maximum at about $\mu = 0.3$ for the symmetric cases (identical supports at both ends), at about $\mu = 0.5$ for the fixed-free case, and about $\mu = 0.4$ for simple-free case. The designer can therefore ensure that operational range of a rotor is well removed from critical speed regions by a judicious selection of in-span support position.

A similar exercise can be carried out for other multi-span rotors. The advantage of having this efficient means of evaluating critical speeds for different configurations is obvious.

Table 7: Results for two cases of non-uniform rotors (as shown in Table 7) are given. These are based on the characteristic value of Re_1. Values for rotors with small and large Re's are presented. As before, values for small Re are seen to be close to Euler beam results while there is significant change from these for large Re.

CHAPTER 6

CONCLUSIONS

Transfer Finite Element Method has been applied successfully for determining natural frequencies and critical speeds of rotors in a variety of situations. This method offers the advantage of reduced computer memory requirement vis-a-vis standard Finite Element Method. It is hence a useful technique for solving such problems in rotor dynamics.

TABLE 1

Convergence Study for Various Rotors

(One governing differential equation, Re = 0.05, Mc = 2.9)

1. Simple-simple

Mode	Number of elements				
	4	6	8	12	Exact [1]
1	9.641	9.639	9.638	9.638	9.638
2	36.014	35.905	35.886	35.878	35.876
3	73.343	72.399	72.224	72.152	72.135
4	122.897	113.415	112.656	112.342	112.261

2. Cantilever

Mode	Number of elements			
	4	6	8	12
1	3.477	3.477	3.477	3.475
2	20.460	20.444	20.441	20.439
3	52.196	51.951	51.902	51.880
4	90.805	90.088	89.801	89.676

Continued....

TABLE 1 (Continued):

3. Fixed-fixed

Mode	Number of elements			
	4	6	8	12
1	21.687	21.666	21.660	21.660
2	55.111	54.750	54.682	54.656
3	95.959	95.219	94.827	94.661
4	153.642	138.135	136.970	136.397

TABLE 2

Convergence Study for Various Rotors

(Two governing differential equations, Re = 0.05, Mc = 2.9)

1. Simple-simple

Mode	Number of elements					
	6	9	12	15	18	Exact [
1	9.746	9.570	9.510	9.482	9.467	9.638
2	37.960	35.569	34.779	34.423	34.231	35.876
3	83.398	73.479	70.307	68.895	68.142	72.135
4	144.764	120.582	112.599	109.072	107.201	112.261

2. Fixed-fixed

Mode	Number of elements				
	6	9	12	15	18
1	20.334	19.586	19.335	19.221	19.159
2	52.381	48.126	46.735	46.109	45.774
3	97.434	85.319	81.354	79.583	78.635
4	153.792	129.629	121.149	117.348	115.319

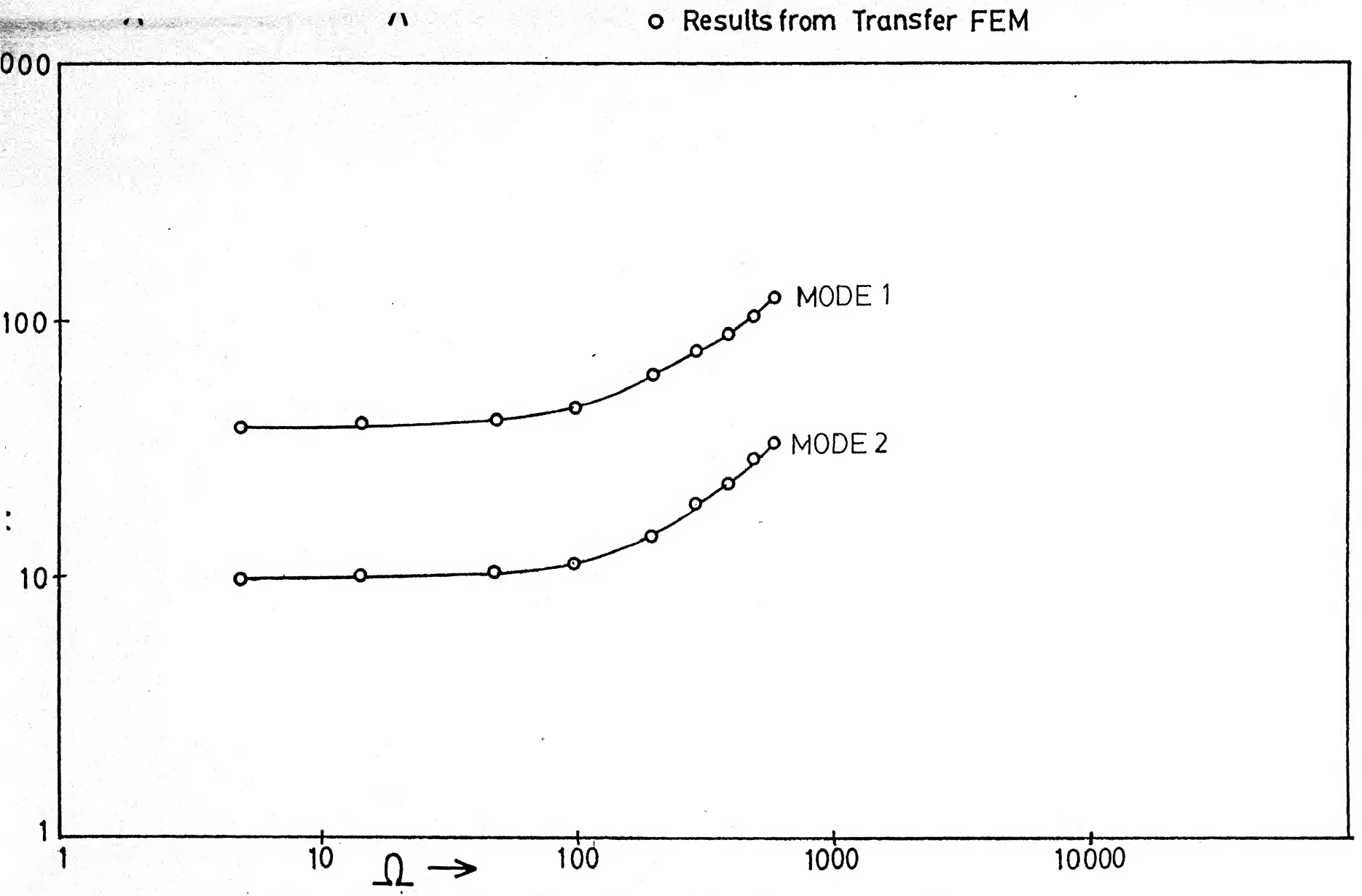

FIG 5.1 Natural Frequency λ vs Rotor Speed Ω

For Rotor Without Shear Effects

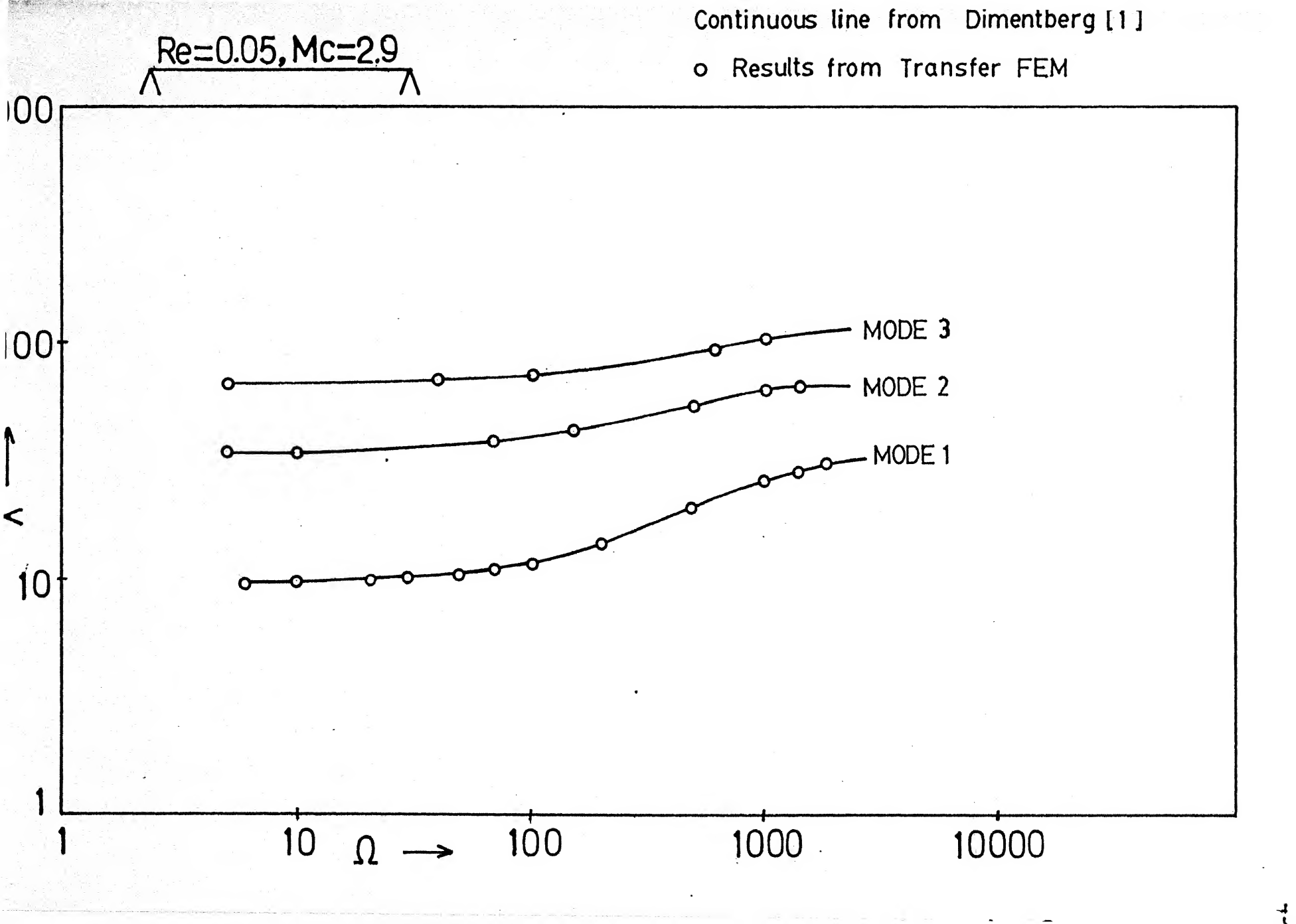
Continuous line from Dimentberg [1]
o Results from Transfer FEM
Re=0.05, Mc=2.9
100
10
1
MODE 3
MODE 2
MODE 1
1
10
Ω
100
1000
10000

TABLE 3

Critical Speeds from one and two Governing Equations Approach

($Re_L = 0.05$, $Re_S = 0.0125$, $Mc = 2.9$)

Notes: i) Columns numbered 1 and 2 contain results from one and two governing equations respectively

ii) 8 elements considered for one equation approach while 12 elements considered for two equation approach

1. Simple-simple

Mode	Re_L		Re_S	
	1	2	1	2
1	9.638	9.510	9.855	9.925
2	35.886	34.779	39.257	40.336
3	72.224	70.307	87.767	93.374
4	112.656	112.599	154.811	172.535

2. Cantilever

Mode	Re_L		Re_S	
	1	2	1	2
1	3.477	3.442	3.513	3.514
2	20.441	19.508	21.931	22.191
3	51.902	48.792	61.030	63.244
4	89.801	85.119	118.620	127.508

Continued.

TABLE 3 (Continued):

3. Fixed-fixed

Mode	Re_L		Re_S	
	1	2	1	2
1	21.660	19.335	23.336	22.580
2	54.682	46.735	61.286	63.520
3	94.827	81.354	119.392	128.381
4	136.970	121.149	195.836	221.439

TABLE 4

Comparison of Critical Speeds for Small and Large Re Values

(Re_S = 0.0125, Re_L = 0.05, Mc = 2.9, 8 elements)

1. Simple-simple

Mode	Euler [18]	Re_S		Re_L	
		Timoshenko	Rotor	Timoshenko	Rotor
1	9.87	9.84	9.85	9.43	9.64
2	39.48	39.02	39.25	33.81	35.89
3	88.83	86.65	87.76	66.56	72.22
4	157.90	151.53	154.81	103.51	112.66

2. Cantilever

Mode	Euler [18]	Re_S		Re_L	
		Timeshenko	Rotor	Timoshenko	Rotor
1	3.52	3.51	3.51	3.44	3.48
2	22.03	21.82	21.93	19.25	20.44
3	61.70	60.34	61.03	47.33	51.90
4	120.91	116.25	118.62	81.09	89.80

Continued.....

TABLE 4 (Continued):

3. Fixed-fixed

Mode	Euler [18]	Re_S		Re_L	
		Timeshenko	Rotor	Timoshenko	Rotor
1	22.37	22.29	23.34	21.22	21.66
2	61.67	60.87	61.29	52.11	54.68
3	120.91	117.75	119.39	89.90	94.83
4	199.86	191.55	195.84	131.08	136.97

TABLE 5

Natural Frequencies/Critical Speeds for Some Multi-span Cases

(Re = 0.05, Mc = 2.9)

Double-span:

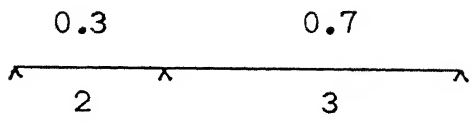

Mode	Euler beam		Rotor
	Exact [18]	Present	
1	26.01	26.37	24.95
2	85.56	87.09	70.62
3	138.06	140.75	104.22
4	201.64	228.52	138.36

Triple-span:

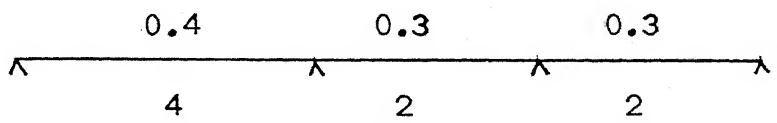

Mode	Euler beam		Rotor
	Exact [18]	Present	
1	26.23	26.23	23.88
2	107.54	107.60	86.40
3	161.80	162.76	111.91
4	228.61	230.95	142.26

Continued.

TABLE 5 (Continued):

Four-span:

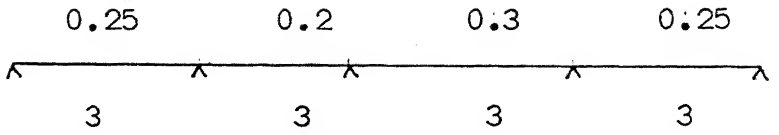

Mode	Euler beam		Rotor
	Exact [18]	Present	
1	36.07	36.08	31.69
2	158.26	158.49	112.63
3	195.72	195.99	133.25
4	298.60	299.34	162.73

TABLE 6

Variation in Critical Speeds of Double Span Rotors with Change in Position of In-span Support

(Re = 0.0125)

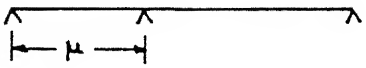

Mode	μ				
	0.1	0.2	0.3	0.4	0.5
1	17.83	21.28	26.25	33.29	39.25
2	57.80	69.75	84.99	76.09	61.24

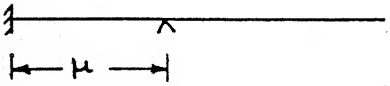

Mode	μ				
	0.2	0.4	0.5	0.6	0.8
1	4.90	7.53	9.85	13.52	21.83
2	31.13	49.94	60.95	51.87	51.82

Continued....

TABLE 6 (Continued):

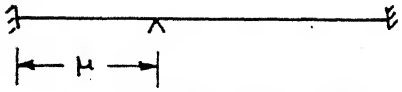

Mode	μ				
	0.1	0.2	0.3	0.4	0.5
1	26.91	31.91	39.53	50.86	61.24
2	72.20	88.09	109.24	111.18	88.80

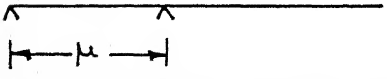

Mode	μ				
	0.2	0.4	0.5	0.6	0.8
1	4.75	7.05	9.05	11.98	14.57
2	30.46	47.00	46.24	36.65	44.96

TABLE 7

Critical Speeds for Non-uniform Rotors

(Results based on characteristic value of Re_1)

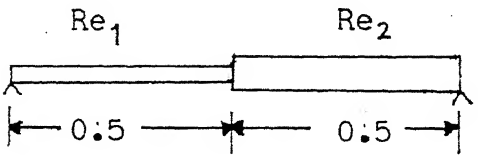

$Re_S \Rightarrow Re_1 = 0.025, Re_2 = 0.0$

$Re_L \Rightarrow Re_1 = 0.05, Re_2 = 0.0$

Mode	Euler	Re_S	Re_L
1	10.89	10.80	10.56
2	44.35	43.05	39.35
3	98.32	91.90	76.31

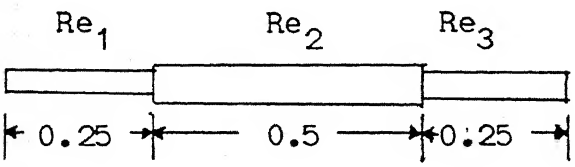

$Re_S \Rightarrow Re_1 = Re_3 = 0.025, Re_2 = 0.0$

$Re_L \Rightarrow Re_1 = Re_3 = 0.05, Re_2 = 0.0$

Mode	Euler	Re_S	Re_L
1	11.75	11.67	11.44
2	43.55	42.26	38.62
3	96.85	90.31	74.77

APPENDIX A

NON-DIMENSIONALISED GOVERNING DIFFERENTIAL EQUATIONS

Characteristic length : L

Characteristic time, $T_* = (mL^4/EI)^{1/2}$ where $m = \rho A$

Non-dimensional variables used are therefore:

$$Z = z/L,\ S = s/L,\ T = t/T_*, \Omega = \omega . T_*$$

Then

$$\frac{\partial^n z}{\partial s^n} = \frac{1}{L^{(n-1)}} \cdot \frac{\partial^n Z}{\partial S^n} \quad , \quad \frac{\partial^n z}{\partial t^n} = \frac{L}{T_*^n} \cdot \frac{\partial^n Z}{\partial T^n}$$

$$\frac{\partial \Psi}{\partial s} = \frac{1}{L} \cdot \frac{\partial \Psi}{\partial S} \quad , \quad \frac{\partial^n \Psi}{\partial t^n} = \frac{1}{T_*^n} \cdot \frac{\partial^n \Psi}{\partial T^n}$$

A1. Two-governing Differential Equations

Equations (2.2.3) are:

$$m\ddot{z} - \frac{\partial}{\partial s}\left[k'GA\ (z' - \Psi)\right] = 0$$

$$\frac{\partial}{\partial s}(EI\ \Psi') + k'GA\ (z' - \Psi) - mk^2 \ddot{\Psi} + 2imk^2 \omega \dot{\Psi} = 0$$

Using non-dimensional variables and expressions the above equations become:

$$-\frac{mL}{T_*^2} \frac{\partial^2 Z}{\partial T^2} + \frac{1}{L} \frac{\partial}{\partial S}\left[k'GA\left(\frac{\partial Z}{\partial S} - \Psi\right)\right] = 0$$

$$-\frac{1}{L} \cdot \frac{\partial}{\partial S}\left(\frac{EI}{L} \frac{\partial \Psi}{\partial S}\right) + k'GA\left(\frac{\partial Z}{\partial S} - \Psi\right) - \frac{mk^2}{T_*^2} \frac{\partial^2 \Psi}{\partial T^2} + 2i \frac{mk^2}{T_*^2} \Omega \frac{\partial \Psi}{\partial T}$$

For a uniform rotor section, k'GA and EI are constants. The above equation can hence be rewritten as:

$$(Z'' - \Psi') - Mc.Re^2 . \ddot{Z} = 0$$

$$\Psi'' + \frac{1}{Mc.Re^2} (Z' - \Psi) - Re^2 (\ddot{\Psi} - 2i\Omega \dot{\Psi}) = 0$$

where Mc is the non-dimensional material constant, E/k'G, and Re (also non-dimensional) is the rotary inertia factor, k/L. Mc accounts for shear effects while Re accounts for rotary inertia of elements and also contributes to the gyroscopic action term (since polar moment of inertia is taken to be twice equatorial moment of inertia for a circular disc for equation (2.2.3)).

The above is presented as equation (2.2.4) in Chapter 2.

A.2. Single-governing Differential Equation

Equation (2.3.3) is

$$\frac{EI}{m} z^{IV} - k^2 (1 + \frac{E}{k'G}) \ddot{z}'' + 2i\omega k^2 \dot{z}'' + \ddot{z} + \frac{mk^2}{k'GA} \dddot{z} - 2i\omega \frac{mk^2}{k'GA} \dddot{z} = 0$$

Using non-dimensionalised parameters one obtains:

$$\frac{EI}{mL^3} \cdot \frac{\partial^4 Z}{\partial S^4} - k^2 \left(1 + \frac{E}{k'G}\right) \cdot \frac{1}{LT_*^2} \frac{\partial^{"} Z}{\partial S^2 \partial T^2}$$

$$+ 2i\Omega \; k^2 \frac{1}{LT_*^2} \frac{\partial^3 Z}{\partial S^2 \, \partial T} + \frac{L}{T_*^2} \cdot \frac{\partial^2 Z}{\partial T^2} + \frac{mk^2}{k'GA} \cdot \frac{L}{T_*^4} \frac{\partial^4 Z}{\partial T^4}$$

$$- 2i\Omega \frac{mk^2}{k'GA} \frac{L}{T_*^4} \frac{\partial^3 Z}{\partial T^3} = 0 \; .$$

Dividing the equation by (L/T^2_*) and simplifying expressions:

$$Z^{IV} - Re^2 (1+Mc) \dot{Z}^{"} + 2i\Omega . Re^2 . \dot{Z}^{"} + Mc . Re^4 . \dot{Z}^{....}$$

$$+ \ddot{Z} - 2i\Omega . Mc . Re^4 . \dot{Z}^{...} = 0$$

with Mc and Re as defined above (Sec. A.1) . This is presented as equation (2.3.4) in Chapter 2.

APPENDIX B

FINITE ELEMENT FORMULATION FOR TWO GOVERNING EQUATION APPROACH

For a finite element, governing equations from equation (2.2.4) are:

$$(Z'' - \Psi') - C_1 \cdot \dot{Z} = 0 \qquad \text{(B.1a)}$$

$$\Psi'' + \frac{1}{C_1}(Z' - \Psi) - C_2 (\dot{\Psi} - 2i\Omega\Psi) = 0 \qquad \text{(B.1b)}$$

where

$'$: derivative w.r.t. local non-dimensional coordinate η (and not w.r.t. S as in equation (2.2.4))

$\cdot$: derivate w.r.t. non-dimensional time T

$C_1 = Mc.Re^2$, $C_2 = Re^2$

$Z = Z(\eta, T)$, $\Psi = \Psi(\eta, T)$.

Assume polynomial solutions for Z and Ψ over the element:

$$Z^{(e)} = \lfloor N^Z \rfloor \{Z\}^{(ne)} \quad , \quad \Psi^{(e)} = \lfloor N^\Psi \rfloor \{\Psi\}^{(ne)}$$

Substituting the above expressions in equations (B.1) will give residues from both equations. Minimising residue from (B.1a) by Galerkin's method using $\lfloor N^Z \rfloor$ and that from (B.1b) using $\lfloor N^\Psi \rfloor$, one gets:

$$- \int_0^H \{N^Z{}'\} \lfloor N^Z{}' \rfloor \, d\eta \, \{Z\}^{(ne)} + \int \{N^Z{}'\} \lfloor N^\Psi \rfloor \, d\eta \, \{\Psi\}^{(ne)}$$

$$- C_1 \int_0^H \{N^Z\} \lfloor N^Z \rfloor \, d\eta \, \{\ddot{Z}\}^{(ne)} = \{N^Z\} \Psi^{(e)} \Big|_0^H$$

$$- \{N^Z\} \frac{\partial Z^{(e)}}{\partial \eta} \Big|_0^H \qquad \text{(B.2a)}$$

$$- \int_0^H \{N^{\Psi'}\} \lfloor N^{\Psi'} \rfloor d\eta \, \{\Psi\}^{(ne)} + \frac{1}{C_1} \int_0^H \{N^\Psi\} \lfloor N^Z{}' \rfloor \, d\eta \{Z\}^{(ne)}$$

$$- \frac{1}{C_1} \int_0^H \{N^\Psi\} \lfloor N^\Psi \rfloor \, d\eta \, \{\Psi\}^{(ne)}$$

$$- C_2 \int_0^H \{N^\Psi\} \lfloor N^\Psi \rfloor \, d\eta \, \{\ddot{\Psi}\}^{(ne)} + 2i \, C_2 \int_0^H \{N^\Psi\} \lfloor N^\Psi \rfloor \, d\eta \{\dot{\Psi}\}^{(}$$

$$= - \{N^\Psi\} \frac{\partial \Psi^{(e)}}{\partial \eta} \Big|_0^H \qquad \text{(B.2b)}$$

Applying the criteria of completeness and compatibility it is seen that interpolating functions for both Z and Ψ need to linear. In terms of shape functions, $[N^Z]$ and $[N]$ therefore become identical and these are [12] :

$$\lfloor N \rfloor = \lfloor 1 - \frac{\eta}{H} \quad \frac{\eta}{H} \rfloor$$

while $$\{Z\}^{(ne)} = \lfloor Z_1 \quad Z_2 \rfloor^T$$

and $$\{\Psi\}^{(ne)} = \lfloor \Psi_1 \quad \Psi_2 \rfloor^T$$

where subscripts 1 and 2 denote values at nodes 1 and 2 of the element (i.e. $\eta = 0$ and H respectively).

Assuming $\{Z\}^{(ne)}$ and $\{\Psi\}^{(ne)}$ of $e^{i\lambda T}$ form, one gets from equations (B.2):

$$[K1]\{Z\}^{(ne)} - [K2]\{\Psi\}^{(ne)} - C_1.\lambda^2.[MM]\{Z\}^{(ne)} = \{N\}\frac{dZ}{d\eta} - \{N\}\Psi\Big|_0^H \qquad (B.3a$$

$$[K3]\{\Psi\}^{(ne)} - \frac{1}{C_1}[K5]\{Z\}^{(ne)} + \frac{1}{C_1}[K4]\{\Psi\}^{(ne)} - C_2.\lambda^2.[MM]\{\Psi\}^{(ne)} + 2\Omega.\lambda.C_2[MM]\{\Psi\}^{(ne)} = N \qquad (B.3$$

where

$$[K1] = \int_0^H \{N'\}\lfloor N'\rfloor d\eta \quad , [K2] = \int_0^H \{N'\}\lfloor N\rfloor d\eta$$

$$[K3] = \int_0^H \{N'\}\lfloor N'\rfloor d\eta = [K1] \quad , [K4] = \int_0^H \{N\}\lfloor N\rfloor d\eta$$

$$[K5] = \int_0^H \{N\}\lfloor N'\rfloor d\eta \quad , [MM] = \int_0^H \{N\}\lfloor N\rfloor d\eta$$

are all square matrices of order 2. Note that while [K1] and are identical, a distinction has been maintained between [K4] a [MM]. This because due to ill-conditioning, reduced integrat by Gaussian quadrature is carried out for [K4]. The elements of these are given in Appendix C.

Equations (B.3) can be written compactly as:

$$\left[[K1] - C_1 \cdot \lambda^2 \cdot [MM]\right]\{Z\}^{(ne)} - [K2]\{\Psi\}^{(ne)} = \begin{Bmatrix} -F_1 \\ F_2 \end{Bmatrix} \qquad \text{(B.4a}$$

$$-\frac{1}{C_1}[K5]\{Z\}^{(ne)} + \left[[K3] + [K4] + (2\Omega\lambda - \lambda^2)[M]\right]$$

$$\{\Psi\}^{(ne)} = \begin{Bmatrix} -M_1 \\ M_2 \end{Bmatrix} \qquad \text{(B.4}$$

where

$$F_i = \left(\frac{dZ}{d\eta} - \Psi\right)\Big|_i \quad \text{and} \quad M_i = \frac{d\Psi}{d\eta}\Big|_i .$$

The above equations can be combined to yield the followin finite element matrix equation:

$$\begin{bmatrix} [K1] - C_1\lambda^2[MM] & -[K2] \\ -\frac{1}{C_1}[K5] & [K3] + [K4] + (2\Omega\lambda - \lambda^2)[MM] \end{bmatrix} \begin{Bmatrix} \{Z_1\} \\ \{Z_2\} \\ \{\Psi_1\} \\ \{\Psi_2\} \end{Bmatrix} = \begin{Bmatrix} \{ - \\ \{ - \end{Bmatrix}$$

APPENDIX C

FINITE ELEMENT MATRICES

C.1

Matrices for four degrees of freedom finite elements

$$[K] = \frac{1}{H^3}\begin{bmatrix} 12 & 6H & -12 & 6H \\ & 4H^2 & -6H & 2H^2 \\ \text{symmetric} & & 12 & -6H \\ & & & 4H^2 \end{bmatrix}$$

$$[M] = \frac{H}{420}\begin{bmatrix} 156 & 22H & 54 & -13H \\ & 4H^2 & 13H & -3H^2 \\ \text{symmetric} & & 156 & -22H \\ & & & 4H^2 \end{bmatrix}$$

$$[MB] = \frac{1}{H}\begin{bmatrix} \frac{6}{5} & \frac{H}{10} & -\frac{6}{5} & \frac{H}{10} \\ & \frac{2H^2}{15} & -\frac{H}{10} & -\frac{H^2}{30} \\ \text{symmetric} & & \frac{6}{5} & -\frac{H}{10} \\ & & & \frac{2H^2}{15} \end{bmatrix}$$

C.2

Matrices for two degree of freedom element:

$$[K1] = [K3] = \frac{1}{H}\begin{bmatrix} 1 & -1 \\ -1 & 1 \end{bmatrix}$$

$$[K2] = \frac{1}{2}\begin{bmatrix} -1 & -1 \\ 1 & 1 \end{bmatrix}$$

$$[K4] = \frac{H}{6}\begin{bmatrix} 2 & 1 \\ 1 & 2 \end{bmatrix}$$ (without reduced integra

$$[K4] = \frac{H}{4}\begin{bmatrix} 1 & 1 \\ 1 & 1 \end{bmatrix}$$ (with reduced integratio

$$[K5] = \frac{1}{2}\begin{bmatrix} -1 & 1 \\ -1 & 1 \end{bmatrix}$$

$$[MM] = \frac{H}{6}\begin{bmatrix} 2 & 1 \\ 1 & 2 \end{bmatrix}$$

REFERENCES

1. Dimentberg, F.M. Flexural Vibrations of Rotating Shafts, Butterworths, London, 1961.

2. Tondl, A. Some Problems of Rotor Dynamics, Chapman and Hall, London, 1965.

3. Rao, J.S. Rotor Dynamics, Wiley Eastern, New Delhi, 1983.

4. Gupta, D.K. Transfer Finite Element Method for Static and Dynamic Problems, M. Tech. Thesis, Department of Mechanical Engineering, Indian Institute of Technology, Kanpur, 1983.

5. Darnley, E.R. The Transverse Vibrations of Beams and the Whirling of Shafts Supported at Intermediate Points, Phil. Mag., Vol. 41, p. 81, 1921.

6. Timoshenko, S. Vibration Problems in Engineering, 3rd ed., D. Van Nostrand, 1956.

7. Tse, F.S., Morse, I.E. and Hinkel, Mechanical Vibrations, Prentice Hall of India, New Delhi, 1974.

8. Patnaik, S.K. and Mallik, A.K. Natural Frequencies of a Shaft with Periodically Placed Rotors and Bearings, J. of Sound and Vibration, Vol. 85, No. 3, pp.415-422, 1982.

9. Pestel, E.C. and Leckie, F.A. Matrix Methods in Elastomechanics, McGraw-Hill, New York, 1963.

10. Pilkey, W.D. and Chang, P.Y. Modern Formulas for Statics and Dynamics, McGraw-Hill, New York, 1978.

11. Subramanya, K. Flexibility Analysis of Pipes by Transfer Finite Element Method, Department of Mechanical Engineering, Indian Institute of Technology, Kanpur, 1985.

12. Cook, R.D. Concepts and Applications of Finite Element Analysis, 2nd ed., John Wiley & Sons, 1974.

13. Meirovitch, L. Analytical Methods in Vibrations, Collier-Macmillan, London, 1967.

14. Thomas, J. and Abbas, B.A.H. Finite Element Model for Dynamic Analysis of Timoshenko Beam, J. of Sound and Vibration, Vol. 41, No.3, pp. 291-299, 1975.

15. Singh, K. and Singh, B.P. In-plane Vibrations of Rotating Sectors and Rings with and without Radial supports by Finite Element Method, Computers and Structures, Vol. 19, No.4, pp.545-554, 1984.

16. Huebner, K.H. The Finite Element Method for Engineers, 2nd ed., John Wiley & Sons, 1983.

17. Shigley, J.E. Mechanical Engineering Design, 3rd ed., McGraw Hill, 1977.

18. Gorman, D.J. Free Vibration Analysis of Beams and Shafts, John Wiley & Sons, 1975.

19. Gallagher, R.H. Finite Element Analysis Fundamentals, Prentice Hall, 1975.

20. Zeinckiwicz, O.C. The Finite Element Method, Tata McGraw-Hill, New Delhi, 1979.

21. Dym, C.L. and Shames, I.H. Solid Mechanics: A Variational Approach, McGraw-Hill, 1973.

Date Slip

This book is to be returned on the date last stamped.
